

Online Convolutional Sparse Coding with Sample-Dependent Dictionary

Yaqing Wang, *Member IEEE*, Quanming Yao, *Member IEEE*, James T. Kwok, *Fellow IEEE*,
and Lionel M. Ni, *Fellow IEEE*

Abstract

Convolutional sparse coding (CSC) has been popularly used for the learning of shift-invariant dictionaries in image and signal processing. However, existing methods have limited scalability. In this paper, instead of convolving with a dictionary shared by all samples, we propose the use of a sample-dependent dictionary in which filters are obtained as linear combinations of a small set of base filters learned from the data. This added flexibility allows a large number of sample-dependent patterns to be captured, while the resultant model can still be efficiently learned by online learning. Extensive experimental results show that the proposed method outperforms existing CSC algorithms with significantly reduced time and space requirements.

I. INTRODUCTION

In recent years, convolutional sparse coding (CSC) [38] has been used successfully in image processing [14], [15], [30] signal processing [10], and biomedical applications [2], [3], [8], [26]. It is closely related to sparse coding [1], [20], but the dictionary in CSC is shift-invariant and can capture shifted local patterns that are common in signals and images. In CSC, each data sample is then represented by the sum of a set of filters from the dictionary convolved with the corresponding codes.

Traditionally, the CSC algorithms operate in batch mode [18], [38], [27], [7], [15], [32], [35], and one needs to access and process all the samples and codes in each iteration. This is expensive, in terms of both space and time, when data sets are large.

Motivated by an efficient online algorithm for sparse coding [23], a number of online learning algorithms have been recently proposed to improve the scalability of CSC [12], [22], [33]. As data samples arrive, relevant information is compressed into small history statistics, and the model is incrementally updated. The samples can then be discarded, leading to a significant reduction in the time and space complexities. For example, consider the OCSC algorithm proposed in [33], which is the most successful among existing online CSC algorithms. It has a time complexity of $O(K^2P + KP \log P)$ (where K is the number of filters, P is the number of elements per sample) and a space complexity of $O(K^2P)$, which is even independent of sample size. These are much smaller than the $O(NK^2P + NKP \log P)$ (for time) and $O(NKP)$ (for space) requirements of batch CSC algorithms, where N is the number of samples.

However, as the space complexity of OCSC still depends quadratically on the number of filters, it cannot learn with a large number of filters. The number of local patterns that can be captured is thus limited, and this may lead to inferior performance, especially on higher-dimensional data sets.

The use of more filters, while being capable of achieving better performance, also leads to a larger number of expensive convolution operations. This can prevent CSC from being used in many practical settings. Rigamonti *et al.* [29] and Sironi *et al.* [31] proposed to post-process the learned set of filters by approximating them by separable filters which can be factorized into one-dimensional filters, making the convolution cheaper to perform. However, as learning and post-processing are then two independent procedures, the resultant filters may not be optimal. Moreover, those separate filters can not be online updated with the arrival of new samples.

Another direction for scaling up CSC is via distributed computation [5]. By distributing the data and workload onto multiple machines, the recent consensus CSC (CCSC) algorithm [9] can handle large, higher-dimensional data

Y. Wang and J. T. Kwok are with Department of Computer Science and Engineering, Hong Kong University of Science and Technology University, Hong Kong.

Q. Yao is with Department of Computer Science and Engineering, Hong Kong University of Science and Technology University, Hong Kong and 4Paradigm Inc., Beijing, China

L.M. Ni is with Department of Computer and Information Science, University of Macau, Macau.

sets such as videos, multispectral images and light field images. However, the heavy computational demands of the CSC problem are only shared over the computing platform, but not fundamentally reduced.

Instead of convolving with a dictionary shared by all samples as in standard CSC, we propose that each sample can have a ‘‘personal’’ dictionary, in which filters are obtained as linear combinations of a small set of base filters learned from the data. As more sample-dependent patterns can be captured by individual personal dictionaries, this added flexibility leads to better performance. Computationally, this hierarchical structure also allows efficient online learning algorithms to be developed. Specifically, the base filter can be updated by the alternating direction method of multipliers (ADMM), while the codes and combination weights can be learned by accelerated proximal algorithms. Extensive experiments on a variety of data sets show that the proposed algorithm outperforms existing (batch, online and distributed) CSC algorithms, and with significant reductions in both time and space.

The rest of the paper is organized as follows. Section II briefly reviews convolutional sparse coding. Section III describes the proposed algorithm. Experimental results are presented in Section IV, and the last section gives some concluding remarks.

Notations: For a vector a , its i th element be $a(i)$, ℓ_1 -norm is $\|a\|_1 = \sum_i |a(i)|$ and ℓ_2 -norm is $\|a\|_2 = \sqrt{\sum_i a^2(i)}$. The convolution of two vectors a and b is denoted $a*b$. For a matrix A , A^* is its complex conjugate, and $A^\dagger = (A^\top)^*$ its conjugate transpose. The Hadamard product of two matrices A and B is $(A \odot B)(i, j) = A(i, j)B(i, j)$. The identity matrix is denoted I .

$\mathcal{F}(x)$ is the Fourier transform that maps x from the spatial domain to the frequency domain, while $\mathcal{F}^{-1}(x)$ is the inverse operator which maps $\mathcal{F}(x)$ back to x .

II. REVIEW: CONVOLUTIONAL SPARSE CODING

Given samples $\{x_1, \dots, x_N\}$ in \mathbb{R}^P , CSC learns a shift-invariant dictionary $D \in \mathbb{R}^{M \times K}$, with the columns $\{D(:, k)\}$ representing the K filters. Each sample x_i is encoded as $Z_i \in \mathbb{R}^{P \times K}$, with the k th column being the code convolved with filter $D(:, k)$. The dictionary and codes are learned together by solving the optimization problem:

$$\min_{D \in \mathcal{D}, \{Z_i\}} \frac{1}{N} \sum_{i=1}^N \frac{1}{2} \left\| x_i - \sum_{k=1}^K D(:, k) * Z_i(:, k) \right\|_2^2 + \beta \|Z_i\|_1, \quad (1)$$

where the first term measures the signal reconstruction error, $\mathcal{D} = \{D : \|D(:, k)\|_2 \leq 1, \forall k = 1, \dots, K\}$ ensures that the filters are normalized, and $\beta > 0$ is a regularization parameter controlling the sparsity of Z_i 's.

In (1), convolution is performed in the spatial domain. This takes $O(KPM)$ time, and is expensive. On the other hand, performing convolution in the frequency domain takes $O(KP \log P)$ time [24], and is faster for typical choices of M and P in CSC applications. Let $\tilde{x}_i \equiv \mathcal{F}(x_i)$, ${}^1\tilde{D}(:, k) \equiv \mathcal{F}(D(:, k))$ and $\tilde{Z}_i(:, k) \equiv \mathcal{F}(Z_i(:, k))$ be the Fourier-transformed counterparts of x_i , $D(:, k)$ and $Z_i(:, k)$. Problem (1) can be rewritten as [7]

$$\begin{aligned} \min_{\substack{\tilde{D}, V \\ \{\tilde{Z}_i, U_i\}}} \frac{1}{2NP} \sum_{i=1}^N \left\| \tilde{x}_i - \sum_{k=1}^K \tilde{D}(:, k) \odot \tilde{Z}_i(:, k) \right\|_2^2 + \beta \|U_i\|_1 \\ \text{s.t. } \mathcal{F}(V(:, k)) = \tilde{D}(:, k), \\ \|\mathcal{C}(V(:, k))\|_2^2 \leq 1, \\ \mathcal{F}(U_i(:, k)) = \tilde{Z}_i(:, k), k = 1, \dots, K, \end{aligned} \quad (2)$$

where $\{U_i\}$ and V are auxiliary variables, and $\mathcal{C}(\cdot)$ crops the extra $P - M$ dimensions from $V(:, k)$.

Problem (2) can be solved by block coordinate descent, which alternates the updates of $\{\tilde{Z}_i, U_i\}$ (code update) and \tilde{D}, V (filter update). The code/filter update subproblems can be solved by the alternating direction method of multipliers (ADMM) [6], which decouples the spatial domain terms (ℓ_1 -regularizer and constraints) from the loss (which involves convolution in the frequency domain). After obtaining $\{\tilde{Z}_i\}$ and \tilde{D} , they are transformed back to the spatial domain as $Z_i(:, k) = \mathcal{F}^{-1}(\tilde{Z}_i(:, k))$ and $D(:, k) = \mathcal{C}\mathcal{F}^{-1}(\tilde{D}(:, k))$, respectively.

During inference, given the learned dictionary D , the testing sample x_j is reconstructed by $\sum_{k=1}^K D(:, k) * Z_j(:, k)$ where Z_j is the obtained codes.

¹ $D(:, k) \in \mathbb{R}^M$ is first zero-padded to be P -dimensional.

A. Post-Processing for Separable Filters

Filters obtained by CSC are non-separable and subsequent convolutions may be slow. To speed this up, they can be post-processed and approximated by separable filters [29], [31]. Specifically, the learned D is approximated by SW , where $S \in \mathbb{R}^{M \times R}$ contains R rank-1 base filters $\{S(:,1), \dots, S(:,R)\}$, and $W \in \mathbb{R}^{R \times K}$ contains the combination weights. However, such approximation will deteriorate learning performance.

B. Online CSC

On large data sets, batch CSC methods are infeasible as $O(NKP)$ space is required to store the samples and codes. To alleviate this problem, an online CSC algorithm (OCSC) is recently proposed in [33]. Given the Fourier-transformed sample \tilde{x}_t and dictionary \tilde{D}_{t-1} from the last iteration, analogous to (2), the corresponding $\{\tilde{Z}_t, U_t\}$ are obtained as

$$\begin{aligned} \min_{\tilde{Z}, U} \quad & \frac{1}{2P} \left\| \tilde{x}_t - \sum_{k=1}^K \tilde{D}_{t-1}(:,k) \odot \tilde{Z}(:,k) \right\|_2^2 + \beta \|U\|_1 \\ \text{s.t.} \quad & \mathcal{F}(U(:,k)) = \tilde{Z}(:,k), \quad k = 1, \dots, K. \end{aligned} \quad (3)$$

Subsequently, \tilde{D}_t and V_t are updated by solving

$$\begin{aligned} \min_{\tilde{D}, V} \quad & \frac{1}{2tP} \sum_{i=1}^t \left\| \tilde{x}_i - \sum_{k=1}^K \tilde{D}(:,k) \odot \tilde{Z}_i(:,k) \right\|_2^2 \\ \text{s.t.} \quad & \mathcal{F}(V(:,k)) = \tilde{D}(:,k), \quad k = 1, \dots, K, \\ & \|\mathcal{C}(V(:,k))\|_2^2 \leq 1, \quad k = 1, \dots, K. \end{aligned} \quad (4)$$

Directly solving (4) is computationally expensive. The following Proposition reformulates (4) so that only small history statistics is required.

Proposition 1 ([33]). \tilde{D}_t, V_t can be obtained by solving the following optimization problem:

$$\begin{aligned} \min_{\tilde{D}, V} \quad & \frac{1}{2P} \sum_{p=1}^P \tilde{D}(p, :) H_t(:, :, p) \tilde{D}^\dagger(:, p) - 2\tilde{D}(p, :) G_t(:, p) \\ \text{s.t.} \quad & \mathcal{F}(V(:,k)) = \tilde{D}(:,k), \quad k = 1, \dots, K, \\ & \|\mathcal{C}(V(:,k))\|_2^2 \leq 1, \quad k = 1, \dots, K, \end{aligned} \quad (5)$$

where $H_t(:, :, p) = \frac{1}{t} \sum_{i=1}^t \tilde{Z}_i^\top(:, p) \tilde{Z}_i^*(p, :) \in \mathbb{R}^{K \times K}$, and $G_t(:, p) = \frac{1}{t} \sum_{i=1}^t \tilde{x}_i^*(p) \tilde{Z}_i^\top(:, p) \in \mathbb{R}^K$.

Hence, the total space complexity is only $O(K^2P)$, which is independent of N . Moreover, H_t and G_t can be updated incrementally. Problem (5) can then be solved by ADMM. The whole procedure is shown in Algorithm 1.

Two other online CSC reformulations have also been proposed recently. Degraux *et al.* [12] proposed to perform convolution in the spatial domain, and is slow. Liu *et al.* [22] proposed to perform convolution in the frequency domain, but it requires huge sparse matrices which are expensive.

III. ONLINE CSC WITH SAMPLE-DEPENDENT DICTIONARY

Though the OCSC algorithm in [33] scales well with sample size N , its space complexity still depends on K quadratically. This limits the number of filters that can be used and can impact performance (as will be demonstrated in Section IV-C). Motivated by the ideas in Section II-A, we propose to approximate the K filters by R base filters, where $R \ll K$. Note that the separable filters in Section II-A are obtained by post-processing, and may not be optimal. On the other hand, we propose to learn the dictionary directly during signal reconstruction. Moreover, filters in the dictionary are combined from the base filters in a sample-dependent manner.

Algorithm 1 Online convolutional sparse coding (OCSC) [33].

1: **Initialize:** $D_0 \in \mathcal{D}$, $H_0 = \mathbf{0}$, $G_0 = \mathbf{0}$;
2: **for** $t = 1, 2, \dots, T$ **do**
3: draw x_t from $\{x_i\}$;
4: $\tilde{x}_t = \mathcal{F}(x_t)$;
5: obtain \tilde{Z}_t using (3);
6: update $\{H_t(:, :, 1), \dots, H_t(:, :, P)\}$ using \tilde{Z}_t ;
7: update $\{G_t(:, 1), \dots, G_t(:, P)\}$ using \tilde{x}_t and \tilde{Z}_t ;
8: update \tilde{D}_t using (5) by ADMM;
9: **end for**
10: **for** $k = 1, 2, \dots, K$ **do**
11: $D_T(:, k) = \mathcal{C}(\mathcal{F}^{-1}(\tilde{D}_T(:, k)))$;
12: **end for**
output D_T .

A. Problem Formulation

Recall that each x_i in (1) is represented by $\sum_{k=1}^K D(:, k) * Z_i(:, k)$. Let $B \in \mathbb{R}^{M \times R}$, with columns $\{B(:, r)\}$ being the base filters. We propose to represent x_i as:

$$x_i = \sum_{k=1}^K \left(\sum_{r=1}^R W_i(r, k) B(:, r) \right) * Z_i(:, k), \quad (6)$$

where W_i is the matrix for the filter combination weights. In other words, each $D(:, k)$ in (1) is replaced by $\sum_{r=1}^R W_i(r, k) B(:, r)$, or equivalently,

$$D_i = B W_i, \quad (7)$$

which is sample-dependent. As will be seen, this allows the W_i 's to be learned independently (Section III-B). This also leads to more sample-dependent patterns being captured and thus better performance (Section IV-D).

Plugging (7) into the CSC formulation in (1), we obtain

$$\min_{B, \{W_i, Z_i\}} \frac{1}{N} \sum_{i=1}^N f_i(B, W_i, Z_i) + \beta \|Z_i\|_1 \quad (8)$$

$$\text{s.t.} \quad B W_i \in \mathcal{D}, \quad i = 1, \dots, N, \quad (9)$$

$$B \in \mathcal{B}, \quad (10)$$

where

$$f_i(B, W_i, Z_i) \equiv \frac{1}{2} \left\| x_i - \sum_{k=1}^K \left(\sum_{r=1}^R W_i(r, k) B(:, r) \right) * Z_i(:, k) \right\|_2^2,$$

and $\mathcal{B} \equiv \{B : \|B(:, r)\|_2 \leq 1, \forall r = 1, \dots, R\}$.

As B and W_i are coupled together in (9), this makes the optimization problem difficult. The following Proposition decouples B and W_i . All the proofs are in the Appendix.

Proposition 2. For $B \in \mathcal{B}$, we have $B W_i \in \mathcal{D}$ if (i) $W_i \in \mathcal{W}_{\ell_1} \equiv \{W : \|W_i(:, k)\|_1 \leq 1, k = 1, \dots, K\}$, or (ii) $W_i \in \mathcal{W}_{\ell_2} \equiv \{W : \|W_i(:, k)\|_2 \leq 1/\sqrt{R}, k = 1, \dots, K\}$.

For simplicity of notation, we use \mathcal{W} to denote \mathcal{W}_{ℓ_1} or \mathcal{W}_{ℓ_2} . By imposing either one of the above structures on $\{W_i\}$, (8) can be simplified as

$$\min_{B, \{W_i, Z_i\}} \frac{1}{N} \sum_{i=1}^N f_i(B, W_i, Z_i) + \beta \|Z_i\|_1 \quad (11)$$

$$\text{s.t.} \quad B \in \mathcal{B}, \quad \text{and} \quad W_i \in \mathcal{W}, \quad i = 1, \dots, N.$$

Using the learned B , in contrast to previous CSC methods, here we extract both W_j and Z_j from the new sample x_j through (11), which can then be used to reconstruct x_j as $x_j^{\text{rec}} = \sum_{k=1}^K \left(\sum_{r=1}^R W_j(r, k) B_T(:, r) \right) * Z_j(:, k)$.

Remark 1. *Sample-dependent filters have also been recently explored in convolutional neural networks (CNN) [11], where they are named as dynamic filters alternatively. It is shown that CNN these sample-dependent filters outperformed the standard CNN on tasks such as one-shot learning [4], video prediction [11] and image deblurring [17].*

Jia et al. [11] needs to use a specially designed neural network to learn the filters, and does not consider the CSC model. On the other hand, the sample-dependent filters here are integrated into the CSC formulation. Moreover, as will be seen in section III-B, learning can be performed easily and effectively in an online setting, with low time and space requirements.

B. Online Learning Algorithm for (11)

As in Section II-B, we propose an online algorithm for better scalability. At the t th iteration, consider

$$\begin{aligned} \min_{B, \{W_i, Z_i\}} \quad & \frac{1}{t} \sum_{i=1}^t f_i(B, W_i, Z_i) + \beta \|Z_i\|_1 \\ \text{s.t.} \quad & B \in \mathcal{B}, \text{ and } W_i \in \mathcal{W}, i = 1, \dots, N. \end{aligned} \quad (12)$$

First, note that the number of convolutions in (6) can be reduced from K to R by rewriting x_i as $\sum_{r=1}^R B(:, r) * (\sum_{k=1}^K W_i(r, k) Z_i(:, k))$. Moreover, as discussed in Section II, it is more efficient to perform convolutions in the frequency domain. The following key proposition further rewrites (12) such that the base filters can be efficiently updated, as will be seen in Section III-B1.

Proposition 3. *Let ${}^2\tilde{B}(:, r) \equiv \mathcal{F}(B(:, r))$, Problem (12) can be rewritten as*

$$\begin{aligned} \min_{\tilde{B}, \{W_i, Z_i\}} \quad & \frac{1}{t} \sum_{i=1}^t \tilde{f}_i(\tilde{B}, W_i, Z_i) + \beta \|Z_i\|_1 \\ \text{s.t.} \quad & \|\mathcal{C}(\mathcal{F}^{-1}(\tilde{B}(:, r)))\|_2 \leq 1, r = 1, \dots, R, \\ & W_i \in \mathcal{W}, i = 1, \dots, N, \end{aligned} \quad (13)$$

where $\tilde{f}_i(\tilde{B}, W_i, Z_i) \equiv \frac{1}{2^P} \|\tilde{x}_i - \sum_{r=1}^R \tilde{B}(:, r) \odot \tilde{Y}_t(:, r)\|_2^2$, and $\tilde{Y}_t(:, r) \equiv \mathcal{F}(Z_t W_t^\top(:, r))$. The spatial-domain base filters can then be recovered as $B(:, r) = \mathcal{C}\mathcal{F}^{-1}(\tilde{B}(:, r))$.

Note that only R (frequency-domain) convolutions are needed for each \tilde{x}_i . Moreover, recall that OCSC requires $O(K^2P)$ space. In contrast, Proposition 3 compresses the information within W_t and Z_t to $\tilde{Y}_t \in \mathbb{R}^{P \times R}$, and the total size ($O(R^2P)$) is much smaller.

1) *Obtaining \tilde{B}_t :* From (13), \tilde{B}_t can be obtained by solving the subproblem:

$$\begin{aligned} \min_{\tilde{B}} \quad & \frac{1}{2tP} \sum_{i=1}^t \left\| \tilde{x}_i - \sum_{r=1}^R \tilde{B}(:, r) \odot \tilde{Y}_t(:, r) \right\|_2^2 \\ \text{s.t.} \quad & \|\mathcal{C}(\mathcal{F}^{-1}(\tilde{B}(:, r)))\|_2 \leq 1, r = 1, \dots, R. \end{aligned} \quad (14)$$

As in Section II, we introduce an auxiliary variable \tilde{V} , and transform (14) to

$$\begin{aligned} \min_{\tilde{B}, \tilde{V}} \quad & \frac{1}{2tP} \sum_{i=1}^t \left\| \tilde{x}_i - \sum_{r=1}^R \tilde{B}(:, r) \odot \tilde{Y}_t(:, r) \right\|_2^2 \\ \text{s.t.} \quad & \mathcal{F}(\tilde{V}(:, r)) = \tilde{B}(:, r), r = 1, \dots, R, \\ & \|\mathcal{C}(\tilde{V}(:, r))\|_2 \leq 1, r = 1, \dots, R. \end{aligned}$$

² $B(:, r) \in \mathbb{R}^M$ is first zero-padded to be P -dimensional.

This is of the same form as (4). Hence, analogous to (5), \tilde{B}_t can be obtained as:

$$\begin{aligned} \min_{\tilde{B}, \tilde{V}} \quad & \frac{1}{2tP} \sum_{i=1}^t \sum_{p=1}^P \tilde{B}(p, :) \tilde{H}_t(:, :, p) \tilde{B}^\dagger(:, p) - 2\tilde{B}(p, :) \tilde{G}_t(:, p) \\ \text{s.t.} \quad & \mathcal{F}(\tilde{V}(:, r)) = \tilde{B}(:, r), r = 1, \dots, R, \\ & \|\mathcal{C}(\tilde{V}(:, r))\|_2 \leq 1, r = 1, \dots, R, \end{aligned} \quad (15)$$

where $\tilde{H}_t(:, :, p) = \frac{1}{t} \sum_{i=1}^t \tilde{Y}_i^\top(:, p) \tilde{Y}_i^*(p, :) \in \mathbb{R}^{R \times R}$, and $\tilde{G}_t(:, p) = \frac{1}{t} \sum_{i=1}^t \tilde{x}_i^*(p) \tilde{Y}_i^\top(:, p) \in \mathbb{R}^R$. They can be incrementally updated as

$$\tilde{H}_t(:, :, p) = \frac{t-1}{t} \tilde{H}_{t-1}(:, :, p) + \frac{1}{t} \tilde{Y}_t^\top(:, p) \tilde{Y}_t^*(p, :), \quad (16)$$

$$\tilde{G}_t(:, p) = \frac{t-1}{t} \tilde{G}_{t-1}(:, p) + \frac{1}{t} \tilde{x}_t^*(p) \tilde{Y}_t^\top(:, p). \quad (17)$$

Problem (15) can then be solved using ADMM as in (5).

TABLE I

COMPARING THE PROPOSED CSCSD ALGORITHM WITH OTHER SCALABLE CSC ALGORITHMS ON PER ITERATION COST. FOR CCSC, THE COST IS MEASURED PER MACHINE, AND L IS THE NUMBER OF MACHINES IN THE DISTRIBUTED SYSTEM. USUALLY, $N \gg K \gg R$, AND $P \gg M$.

	space	code update time	filter update time
OCSC [33]	$O(K^2P)$	$O(KP + KP \log P)$	$O(K^2P + KP \log P)$
OCDL-Degraux [12]	$O(K^2M^2 + KPM)$	$O(K^2P^3)$	$O(K^2PM^2 + KPM)$
OCDL-Liu [22]	$O(K^2P)$	$O(KP + KP \log P)$	$O(K^2P + KP \log P)$
CCSC [9]	$O(\frac{NKP}{L} + KP)$	$O(\frac{NKP}{L} + NKP \log(\frac{P}{L}))$	$O(\frac{NK^2P}{L} + \frac{NKP}{L} \log(\frac{P}{L}))$
CSCSD	$O(R^2P)$	$O(RKP + RP \log P)$	$O(R^2P + RP \log P)$

2) *Obtaining W_t and Z_t* : With the arrival of x_t , we fix the base filters to \tilde{B}_{t-1} learned at the last iteration, and obtain (W_t, Z_t) from (13) as:

$$\min_{W, Z} F(W, Z) \equiv \tilde{f}_t(\tilde{B}_{t-1}, W, Z) + I_{\mathcal{W}}(W) + \beta \|Z\|_1. \quad (18)$$

Here, $I_{\mathcal{W}}(W)$ is the indicator function on \mathcal{W} (i.e., $I_{\mathcal{W}}(W) = 0$ if $W \in \mathcal{W}$ and ∞ otherwise).

As in the CSC literature, it can be shown that ADMM can also be used to solve (18). However, while CSC's code update subproblem in (3) is convex, here, (18) is nonconvex and existing convergence results for ADMM [34] do not apply.

In this paper, we will instead use the nonconvex and inexact accelerated proximal gradient (niAPG) algorithm [36]. This is a recent proximal algorithm for nonconvex problems. As the regularizers on W and Z in (18) are independent, the proximal step w.r.t. the two blocks can be performed separately as: $(\text{prox}_{I_{\mathcal{W}}(\cdot)}(W), \text{prox}_{\beta \|\cdot\|_1}(Z))$ [28]. As shown in [13], [28], these individual proximal steps can be easily computed (for $\mathcal{W} = \mathcal{W}_{\ell_1}$ or \mathcal{W}_{ℓ_2}).

3) *Complete Algorithm*: The whole procedure, which will be called ‘‘Convolutional Sparse Coding with Sample-Dependent Dictionary (CSCSD)’’, is shown in Algorithm 2. Its space complexity, which is dominated by \tilde{H}_t and \tilde{G}_t , is $O(R^2P)$. Its per-iteration time complexity is $O(RKP + RP \log P)$, where the $O(RKP)$ term is due to gradient computation, and $O(RP \log P)$ is due to FFT/inverse FFT. Table I compares its complexities with those of the other online and distributed CSC algorithms. As can be seen, CSCSD has much lower time and space complexities as $R \ll K$.

IV. EXPERIMENTS

Experiments are performed on a number of data sets (Table II). *Fruit* and *City*³ are image data sets that have been commonly used in the CSC literature [38], [7], [15], [27]. We use the default training and testing splits provided in [7]. The images are pre-processed as in [38], [15], [33], which includes conversion to grayscale, feature

³<http://www.cs.ubc.ca/labs/imager/tr/2015/FastFlexibleCSC/>.

Algorithm 2 CSC with Sample-Dependent Dictionary (CSCSD).

```

1: Initialize  $W_0 \in \mathcal{W}$ ,  $B_0 \in \mathcal{B}$ ,  $\bar{H}_0 = \mathbf{0}$ ,  $\bar{G}_0 = \mathbf{0}$ ;
2: for  $t = 1, 2, \dots, T$  do
3:   draw  $x_t$  from  $\{x_i\}$ ;
4:    $\tilde{x}_t = \mathcal{F}(x_t)$ ;
5:   obtain  $W_t, Z_t$  using niAPG;
6:   for  $r = 1, 2, \dots, R$  do
7:      $\tilde{Y}_t(:, r) = \mathcal{F}(Z_t W_t^\top(:, r))$ ;
8:   end for
9:   update  $\{\bar{H}_t(:, :, 1), \dots, \bar{H}_t(:, :, P)\}$  using (16);
10:  update  $\{\bar{G}_t(:, 1), \dots, \bar{G}_t(:, P)\}$  using (17);
11:  update  $\bar{B}_t$  by (15) using ADMM;
12: end for
13: for  $r = 1, 2, \dots, R$  do
14:    $B_T(:, r) = \mathcal{C}(\mathcal{F}^{-1}(\bar{B}_T(:, r)))$ ;
15: end for
output  $B_T$ .

```

standardization, local contrast normalization and edge tapering. These two data sets are small. In some experiments, we will also use two larger data sets, *CIFAR-10*⁴ [19] and *Flower*⁵ [25], that have been used in [33]. Following [15], [33], [27], [9], we set the filter size M as 11×11 .

TABLE II
SUMMARY OF IMAGE DATA SETS USED.

	size	#training	#testing
<i>Fruit</i>	100×100	10	4
<i>City</i>	100×100	10	4
<i>CIFAR-10</i>	32×32	50,000	10,000
<i>Flower</i>	500×500	2,040	6,149

A. Choice of $\mathcal{W} : \mathcal{W}_{\ell_1}$ versus \mathcal{W}_{ℓ_2}

First, we study the choice of \mathcal{W} in Proposition 2. We compare CSCSD-L1, which uses $\mathcal{W} = \mathcal{W}_{\ell_1}$, with CSCSD-L2, which uses $\mathcal{W} = \mathcal{W}_{\ell_2}$. Experiments are performed on *Fruit* and *City*. As in [15], [27], [33], the number of filters K is set to 100. Recall the space complexity results in Table I, we define the compression ratio of CSCSD relative to OCSC (both using the same K) as $\text{CR} = (K/R)^2$. We vary R in $\{K/20, K/10, K/9, \dots, K/2, K\}$, and the corresponding CR is $\{400, 100, 81, \dots, 1\}$. For performance evaluation, we use the testing peak signal-to-noise ratio [27]: $\text{PSNR} = \frac{1}{|\Omega|} \sum_{x_j \in \Omega} 20 \log_{10} \left(\frac{\sqrt{P}}{\|\hat{x}_j - x_j\|_2} \right)$, where \hat{x}_j is the reconstruction of x_j from the testing set Ω .

Results are shown in Figure 1. As can be seen, CSCSD-L1 is much inferior. Figure 2(a) shows the weight W_j obtained with $K = 100$ and $R = 10$ by CSCSD-L1 on a test sample x_j from *City* (results on the other data sets are similar). As can be seen, most of its entries are zero. This is due to the sparsity property of ℓ_1 norm. As typically only one base filter is used to approximate the original filter, the expressive power is severely limited. On the other hand, the W_j learned by CSCSD-L2 has many more nonzero entries (Figure 2(b)). Hence, in the sequel, we will only focus on CSCSD-L2, which will be simply denoted as CSCSD.

B. Sample-Dependent Dictionary

In this experiment, we set $K = 100$, and compare CSCSD with the following algorithms that use sample-independent dictionaries:

⁴<https://www.cs.toronto.edu/~kriz/cifar.html>.

⁵<http://www.robots.ox.ac.uk/~vgg/data/flowers/102/>.

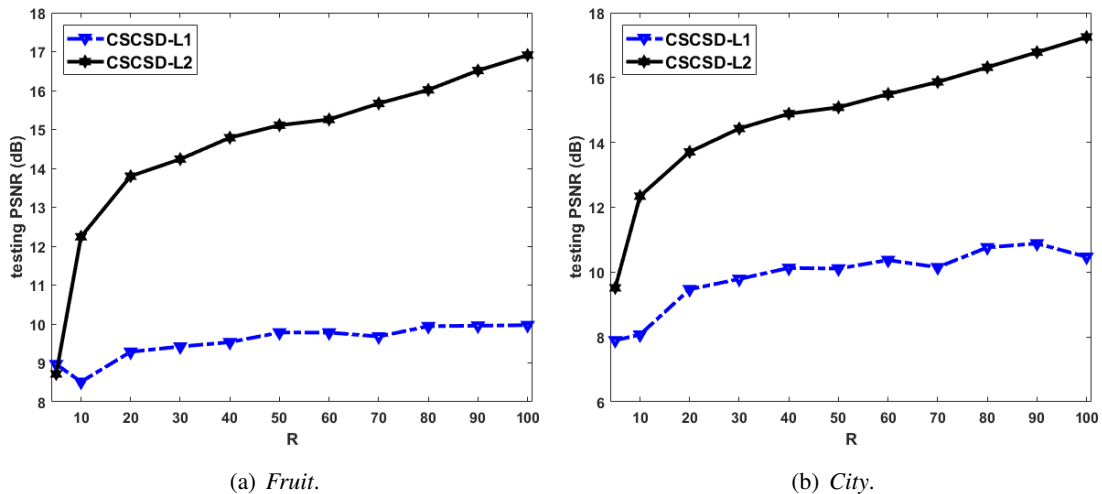


Fig. 1. Testing PSNR's of CSCSD-L1 and CSCSD-L2 at different R 's on the *Fruit* and *City* data sets.

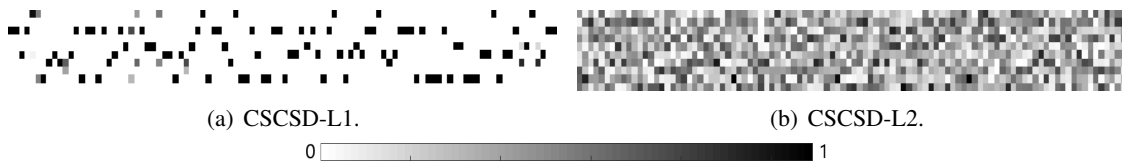


Fig. 2. Weight matrices obtained on a test sample x_j from *City*.

- CSCSD (shared): This is a CSCSD variant in which all W_i 's in (6) are the same. Its optimization is based on alternating minimization.
- Separable filters learned by tensor decomposition (SEP-TD)⁶ [31]: as reviewed in Section II-A, it is based on post-processing the given dictionary (learned by OCSC);
- OCSC⁷: the state-of-the-art in online CSC methods.

Results are shown in Figure 3. As can be seen, CSCSD always outperforms CSCSD(shared) and SEP-TD, and also outperforms OCSC when $R = 10$ (corresponding to $CR = 100$) or above. This demonstrates the advantage of using a sample-dependent dictionary.

Figure 4 compares the sample-dependent dictionary obtained by CSCSD with OCSC's sample-independent dictionary. As can be seen, the CSCSD filters are different for different samples, and can capture local patterns akin to the content of the corresponding sample.

C. Learning with More Filters

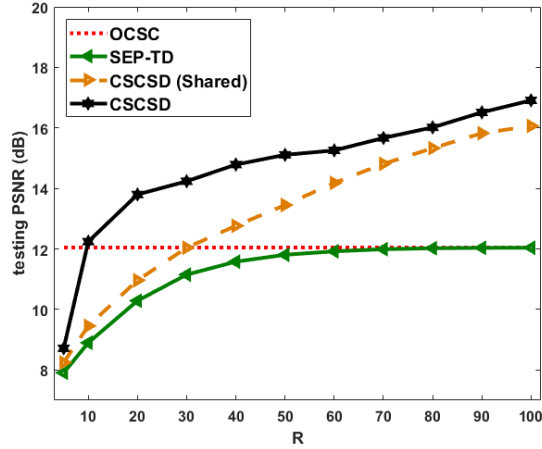
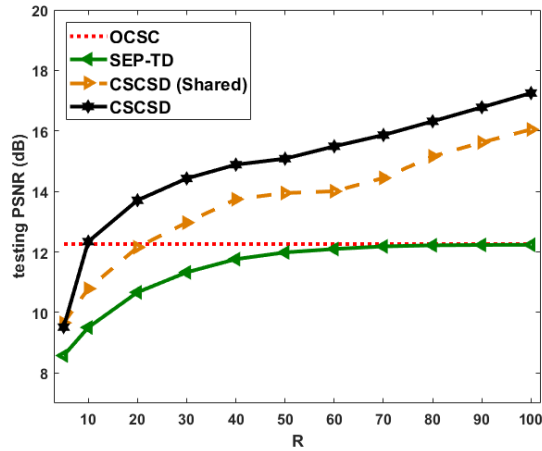
Recall that CSCSD allows the use of more filters (i.e., a larger K). In this Section, we demonstrate that this can lead to better performance. We compare CSCSD with two most recent batch and online CSC methods, namely, slice-based CSC (SBCSC)⁸ [27] and OCSC. For CSCSD, we set $R = 10$ for *Fruit* and *City*, and $R = 30$ for *CIFAR-10* and *Flower*.

Figure 5 shows the testing PSNR's at varying K 's. As can be seen, a larger K consistently leads to better performance for all methods. CSCSD allows the use of a larger K because of its much smaller memory footprint. For example, on *CIFAR-10*, $CR = 1024$ at $K = 800$; on *Flower*, $CR = 1600$ at $K = 400$.

⁶<http://cvlab.epfl.ch/software/filter-learnin>

⁷<http://www.cse.ust.hk/~qyaoaa/code/OCSC.zip>

⁸<http://vardanp.cswp.cs.technion.ac.il/wp-content/uploads/sites/62/2015/12/SliceBasedCSC.rar>

(a) *Fruit*.(b) *City*.Fig. 3. Testing PSNR vs R .

D. Comparison with State-of-the-Art

First, we perform experiments on the two smaller data sets of *Fruit* and *City*, with $K = 100$. We set $R = 10$ (i.e., $\text{CR} = 100$) for CSCSD. This is compared with

- the batch CSC algorithms⁹, including (i) deconvolution networks (DeconvNet) [38], (ii) fast CSC (FCSC) [7], (iii) fast and flexible CSC (FFCSC) [15], (iv) convolutional basis pursuit denoising (CBPDN) [35], (v) the CONSENSUS algorithm [32], and (vi) slice-based CSC (SBCSC) [27]), and
- the online CSC algorithms¹⁰, including OCSC in [33], OCDL-Degraux in [12], and OCDL-Liu in [22]).

Figure 6 shows convergence of the testing PSNR with CPU time. As also demonstrated in [12], [22], [33], online CSC methods converge faster and have better PSNR than batch CSC methods. Among the online methods, CSCSD has comparable PSNR as OCSC, but is faster and requires much less storage ($\text{CR} = 100$).

Next, we perform experiments on the two large data sets, *CIFAR-10* and *Flower*. All the batch CSC algorithms and two online CSC algorithms, OCDL-Degraux and OCDL-Liu, cannot handle such large data sets. Hence, we will only compare CSCSD with OCSC. On *CIFAR-10*, we set $K = 300$, and the corresponding CR for CSCSD is 100.

⁹Codes are obtained from the respective authors: DeconvNet from <http://www.matthewzeiler.com/>, FFCSC from <http://www.cs.ubc.ca/labs/imager/tr/2015/FastFlexibleCSC/>, CBPDN from <http://brendt.wohlberg.net/software/SPORCO/>, and CONSENSUS from <http://zoi.utia.cas.cz/convsparscoding>. Since the FCSC code is no longer available, we use the code in [32] (<http://zoi.utia.cas.cz/convsparscoding>)

¹⁰Since codes for OCDL-Degraux and OCDL-Liu are not available, we implement them according to the paper. Specially, since the code update of OCDL-Degraux ($O(K^2P^3)$) as shown in Table I) is very costly, and the focus here is on filters update, we replace its code update by the one used by OCSC, which explains why OCDL-Degraux is empirically faster than the analyzed complexity.

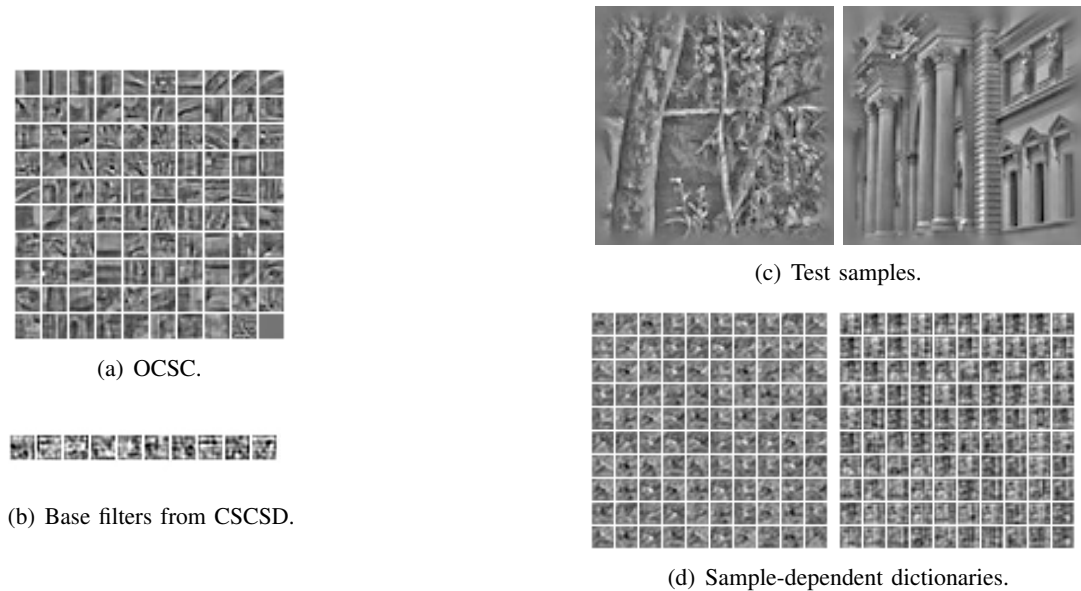


Fig. 4. Dictionaries learned on *City*. As in [1], the filters are sorted in ascending variance. (a) shows the dictionary obtained from OCSC. Using the base filters obtained by CSCSD in (b), (d) shows the sample-dependent dictionaries on the two samples in (c).

On *Flower*, K is still 300 for CSCSD. However, OCSC can only use $K = 50$ because of its much larger memory footprint. Figure 7 shows convergence of the testing PSNR. In both cases, CSCSD significantly outperforms OCSC.

E. Higher-Dimensional Data

In this section, we perform experiments on data sets with dimensionality larger than two. To alleviate the large memory problem, Choudhury *et al.* [9] proposed the use of distributed algorithms. Here, we show that CSCSD can effectively handle these data sets using one single machine.

Experiments are performed on three data sets (Table III) in [9]. The *Video* data set contains image subsequences recorded in an airport [21]. The length of each video is 7, and each image frame is of size 100×100 . The *Multispectral* data contains 60×60 patches from multispectral images (covering 31 wavelengths) of real-world objects and materials [37]. The *Light field* data contains 60×60 patches of light field images on objects and scenes [16]. For each pixel, the light rays are from 8×8 different directions. Following [9], we set the filter size M to $11 \times 11 \times 11$ for *Video*, $11 \times 11 \times 31$ for *Multispectral*, and $11 \times 11 \times 8 \times 8$ for *Light field*.

TABLE III
SUMMARY OF THE HIGHER-DIMENSIONAL DATA SETS USED.

	size	#training	#testing
<i>Video</i>	$100 \times 100 \times 7$	573	143
<i>Multispectral</i>	$60 \times 60 \times 31$	2,200	1,000
<i>Light field</i>	$60 \times 60 \times 8 \times 8$	7,700	385

We compare CSCSD with OCSC and the consensus CSC (CCSC)¹¹ [9] algorithms, with $K = 50$. For fair comparison, only one machine is used for all methods. We do not compare with the batch methods and the two online methods (OCDL-Degraux and OCDL-Liu) as they are not scalable (already shown in Section IV-D).

Because of the small memory footprint of CSCSD, we run it on a GTX 1080 Ti GPU in this experiment. OCSC can also be run on GPU for *Video*. However, *Multispectral* and *Light field* are much larger,¹² and OCSC can only run them on CPU. CCSC, which needs to access all the samples and codes during processing, can only be on CPU.

¹¹https://github.com/vccimaging/CCSC_code_ICCV2017

¹²For *Video*, the memory used (in GB) by CCSC, OCSC, CSCSD (with $R = 5$) and CSCSD (with $R = 10$) are 28.73, 7.58, 2.66, and 2.87. On *Multispectral*, they are 28.26, 11.09, 0.73 and 0.76; on *Light field*, they are 29.79, 15.94, 7.26 and 8.88.

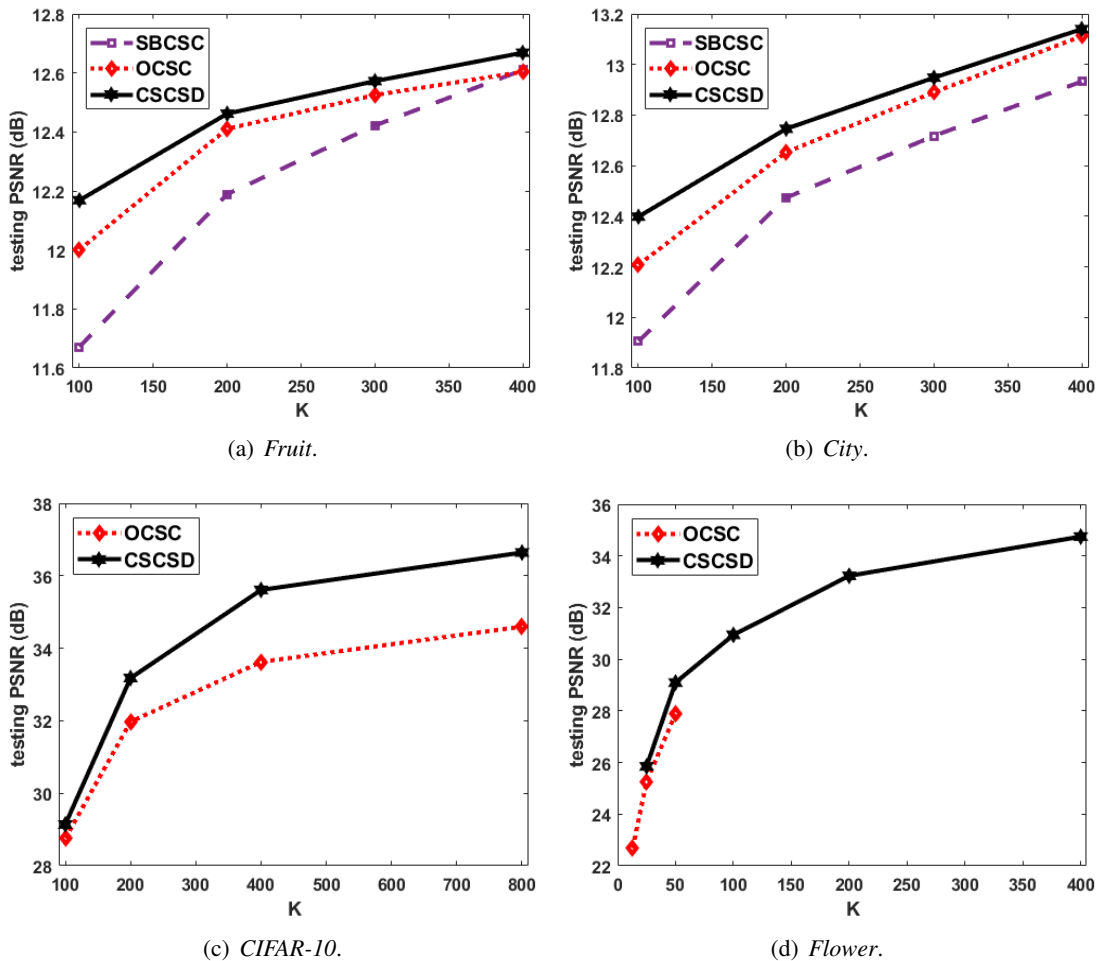


Fig. 5. Effect of K on the testing PSNR. Note that SBCSC cannot be run on *CIFAR-10* and *Flower* which are large. For OCSC, it can run up to $K = 50$ on *Flower*.

Results are shown in Table IV. Since both GPU and CPU are used, we report the clock time instead of CPU time. Note that CSCSD is the only method that can handle the whole of *Video*, *Multispectral* and *Light field* data sets on a single machine. In comparison, CCSC can only handle a maximum of 30 *Video* samples, 40 *Multispectral* samples, and 35 *Light field* samples. OCSC can handle the whole of *Video* and *Multispectral*, but cannot converge in 2 days when the whole *Light field* data set is used. Again, CSCSD outperforms OCSC and CCSC.

TABLE IV
RESULTS ON THE HIGHER-DIMENSIONAL DATA SETS. PSNR IS IN DB AND TIME IS IN HOURS.

	<i>Video</i>		<i>Multispectral</i>		<i>Light field</i>		
	PSNR	time	PSNR	time	PSNR	time	
CCSC	20.4	11.9	17.7	27.8	13.70	9.0	
OCSC	33.0	1.4	30.2	31.2	-	-	
CSCSD	$R=5$	35.0	0.7	30.5	1.2	29.0	11.1
	$\bar{R}=10$	38.0	0.8	31.7	1.4	31.7	18.0

As for speed, CSCSD is the fastest. However, note that this is for reference only as CSCSD is run on GPU while the others (except for OCSC on *Video*) are run on CPU. Nevertheless, this still demonstrates an important advantage of CSCSD, namely that its small memory footprint can benefit from the use of GPU, while the others cannot.

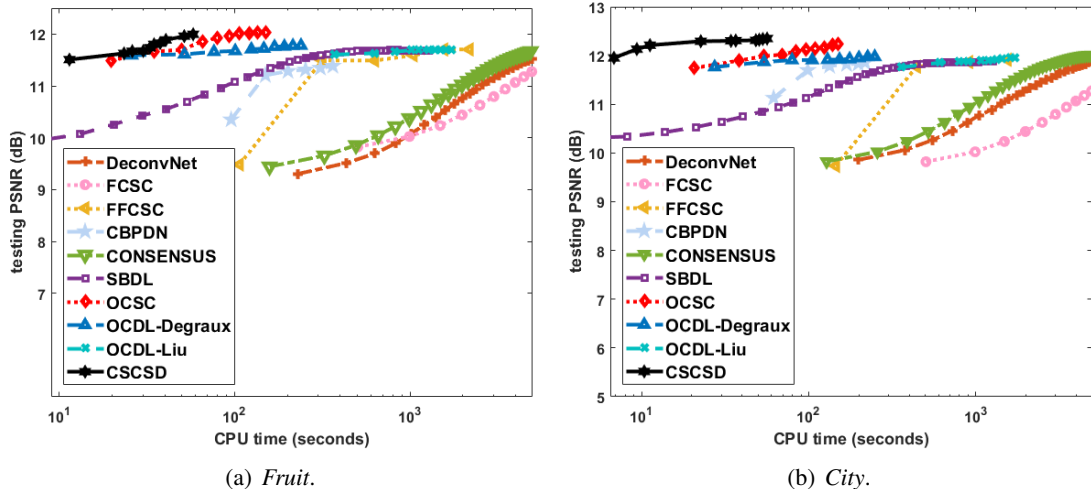


Fig. 6. Testing PSNR on the small data sets.

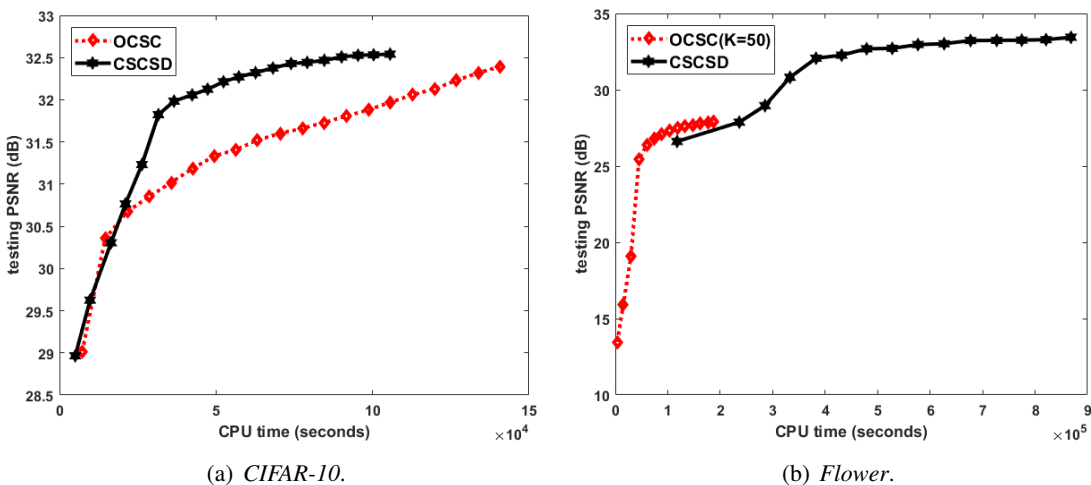


Fig. 7. Testing PSNR on the large data sets.

F. Solving (18): niAPG vs ADMM

Finally, we compare the use of ADMM and niAPG for solving subproblem (18). Experiment is performed on a training sample from *City* in five repetitions. Figure 8 shows convergence of the objective in (18) with time (five repetitions). As can be seen, niAPG has fast convergence while ADMM fails to converge. Besides, ADMM oscillates till the iteration finishes, which shows it does not converge.

V. CONCLUSION

In this paper, we proposed a novel CSC extension, in which each sample has its own sample-dependent dictionary constructed from a small set of shared base filters. Using online learning, the model can be efficiently updated with low time and space complexities. Extensive experiments on a variety of data sets including large image data sets and higher-dimensional data sets all demonstrate its efficiency and scalability.

REFERENCES

- [1] M. Aharon, M. Elad, and A. Bruckstein. K-SVD: An algorithm for designing overcomplete dictionaries for sparse representation. *IEEE Transactions on Signal Processing*, 54(11):4311–4322, 2006.
- [2] F. Andilla and F. Hamprecht. Sparse space-time deconvolution for calcium image analysis. In *Advances in Neural Information Processing Systems*, pages 64–72, 2014.

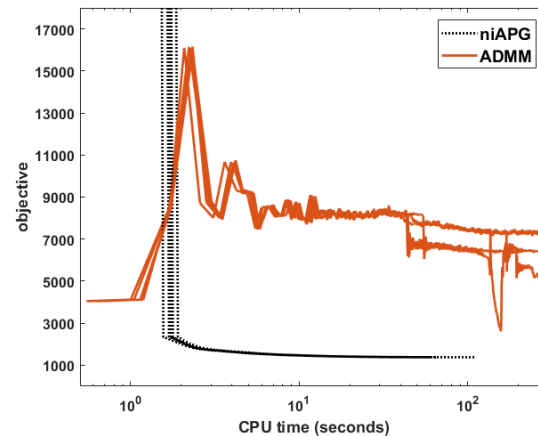


Fig. 8. Convergence of niAPG and ADMM on solving (18).

- [3] R. Annunziata and E. Trucco. Accelerating convolutional sparse coding for curvilinear structures segmentation by refining SCIRD-TS filter banks. *IEEE Transactions on Medical Imaging*, 35(11):2381–2392, 2016.
- [4] L. Bertinetto, J. F. Henriques, J. Valmadre, P. Torr, and A. Vedaldi. Learning feed-forward one-shot learners. In *Advances in Neural Information Processing Systems*, pages 523–531, 2016.
- [5] D. Bertsekas and J. Tsitsiklis. *Parallel and Distributed Computation: Numerical Methods*. Athena Scientific, 1997.
- [6] S. Boyd, N. Parikh, E. Chu, B. Peleato, and J. Eckstein. Distributed optimization and statistical learning via the alternating direction method of multipliers. *Foundations and Trends in Machine Learning*, 3(1):1–122, 2011.
- [7] H. Bristow, A. Eriksson, and S. Lucey. Fast convolutional sparse coding. In *IEEE Conference on Computer Vision and Pattern Recognition*, pages 391–398, 2013.
- [8] H. Chang, J. Han, C. Zhong, A. Snijders, and J. Mao. Unsupervised transfer learning via multi-scale convolutional sparse coding for biomedical applications. *IEEE Transactions on Pattern Analysis and Machine Intelligence*, 2017.
- [9] B. Choudhury, R. Swanson, F. Heide, G. Wetzstein, and W. Heidrich. Consensus convolutional sparse coding. In *Proceedings of the IEEE Conference on Computer Vision and Pattern Recognition*, pages 4280–4288, 2017.
- [10] A. Cogliati, Z. Duan, and B. Wohlberg. Context-dependent piano music transcription with convolutional sparse coding. *IEEE/ACM Transactions on Audio Speech and Language Processing*, 24(12):2218–2230, 2016.
- [11] B. De Brabandere, X. Jia, T. Tuytelaars, and L. Van Gool. Dynamic filter networks. In *Advances in Neural Information Processing Systems*, pages 1–9, 2016.
- [12] K. Degraux, U. S. Kamilov, P. T. Boufounos, and D. Liu. Online convolutional dictionary learning for multimodal imaging. In *IEEE International Conference on Image Processing*, pages –, 2017.
- [13] J. Duchi, S. Shalev-Shwartz, Y. Singer, and T. Chandra. Efficient projections onto the ℓ_1 -ball for learning in high dimensions. In *International Conference on Machine Learning*, pages 272–279, 2008.
- [14] S. Gu, W. Zuo, Q. Xie, D. Meng, X. Feng, and L. Zhang. Convolutional sparse coding for image super-resolution. In *International Conference on Computer Vision*, pages 1823–1831, 2015.
- [15] F. Heide, W. Heidrich, and G. Wetzstein. Fast and flexible convolutional sparse coding. In *IEEE Conference on Computer Vision and Pattern Recognition*, pages 5135–5143, 2015.
- [16] N. K. Kalantari, T. Wang, and R. Ramamoorthi. Learning-based view synthesis for light field cameras. *ACM Transactions on Graphics*, 35(6):193, 2016.
- [17] D. Kang, D. Dhar, and A. Chan. Incorporating side information by adaptive convolution. In *Advances in Neural Information Processing Systems*, pages 3870–3880, 2017.
- [18] K. Kavukcuoglu, P. Sermanet, Y. Boureau, K. Gregor, M. Mathieu, and Y. LeCun. Learning convolutional feature hierarchies for visual recognition. In *Advances in Neural Information Processing Systems*, pages 1090–1098, 2010.
- [19] A. Krizhevsky and G. Hinton. Learning multiple layers of features from tiny images. Technical report, University of Toronto, 2009.
- [20] H. Lee, A. Battle, R. Raina, and A. Ng. Efficient sparse coding algorithms. In *Advances in Neural Information Processing Systems*, pages 801–808, 2007.
- [21] L. Li, W. Huang, I. Y. Gu, and Q. Tian. Statistical modeling of complex backgrounds for foreground object detection. *IEEE Transactions on Image Processing*, 13(11):1459–1472, 2004.
- [22] J. Liu, C. Garcia-Cardona, B. Wohlberg, and W. Yin. Online convolutional dictionary learning. In *IEEE International Conference on Image Processing*, pages –, 2017.
- [23] J. Mairal, F. Bach, J. Ponce, and G. Sapiro. Online learning for matrix factorization and sparse coding. *Journal of Machine Learning Research*, 11:19–60, 2010.
- [24] S. Mallat. *A Wavelet Tour of Signal Processing*. Academic Press, 1999.
- [25] M. Nilsback and A. Zisserman. Automated flower classification over a large number of classes. In *Indian Conference on Computer Vision, Graphics & Image Processing*, pages 722–729, 2008.
- [26] M. Pachitariu, A. Packer, N. Pettit, H. Dalgleish, M. Hausser, and M. Sahani. Extracting regions of interest from biological images with convolutional sparse block coding. In *Advances in Neural Information Processing Systems*, pages 1745–1753, 2013.

- [27] V. Pappas, Y. Romano, J. Sulam, and M. Elad. Convolutional dictionary learning via local processing. In *International Conference on Computer Vision*, pages 5296–5304, 2017.
- [28] N. Parikh and S. Boyd. Proximal algorithms. *Foundations and Trends in Optimization*, 1(3):127–239, 2014.
- [29] R. Rigamonti, A. Sironi, V. Lepetit, and P. Fua. Learning separable filters. In *IEEE Conference on Computer Vision and Pattern Recognition*, pages 2754–2761, 2013.
- [30] A. Serrano, F. Heide, D. Gutierrez, G. Wetzstein, and B. Masia. Convolutional sparse coding for high dynamic range imaging. In *Computer Graphics Forum*, volume 35, pages 153–163, 2016.
- [31] A. Sironi, B. Tekin, R. Rigamonti, V. Lepetit, and P. Fua. Learning separable filters. *IEEE Transactions on Pattern Analysis and Machine Intelligence*, 37(1):94–106, 2015.
- [32] M. Šorel and F. Šroubek. Fast convolutional sparse coding using matrix inversion lemma. *Digital Signal Processing*, 55:44–51, 2016.
- [33] Y. Wang, Q. Yao, J. T. Kwok, and L. M. Ni. Online convolutional sparse coding. Preprint arXiv:1706.06972, 2017.
- [34] Y. Wang, W. Yin, and J. Zeng. Global convergence of ADMM in nonconvex nonsmooth optimization. *arXiv preprint arXiv:1511.06324*, 2015.
- [35] B. Wohlberg. Efficient algorithms for convolutional sparse representations. *IEEE Transactions on Image Processing*, 25(1):301–315, 2016.
- [36] Q. Yao, J. Kwok, F. Gao, W. Chen, and T.-Y. Liu. Efficient inexact proximal gradient algorithm for nonconvex problems. In *International Joint Conferences on Artificial Intelligence*, pages 3308–3314, 2017.
- [37] F. Yasuma, T. Mitsunaga, D. Iso, and S. K. Nayar. Generalized assorted pixel camera: postcapture control of resolution, dynamic range, and spectrum. *IEEE Transactions on Image Processing*, 19(9):2241–2253, 2010.
- [38] M. Zeiler, D. Krishnan, G. Taylor, and R. Fergus. Deconvolutional networks. In *IEEE Conference on Computer Vision and Pattern Recognition*, pages 2528–2535, 2010.